Experimental study of point-defect creation in high-energy heavy-ion tracks

A. Perez
Département de Physique des Matériaux, Université Claude Bernard (Lyon I), 43 boulevard du 11 Novembre 1918, 69622 Villeurbanne CEDEX, France

E. Balanzat and J. Dural
Centre Interdisciplinaire de Recherches avec les Ions Lourds, Grand Accélérateur National d'Ions Lourds (GANIL), 8 boulevard Antoine Henri Becquerel, 14040 Caen CEDEX, France

(Received 5 June 1989)

Thin platelets of LiF crystals have been bombarded on the side with Ne (40 MeV/amu), Ar (60 MeV/amu), Kr (42 MeV/amu), and Xe (27 MeV/amu) ions at room temperature in the dose range from 10^8 to 10^{13} ions cm^{-2}. Taking into account the large penetration depths of these high-energy ions ($\simeq 1.4$, 1.8, 0.6, and 0.2 mm for Ne, Ar, Kr, and Xe, respectively), it was possible to measure the depth distribution profiles of primary point defects (F centers) and aggregated defects (F_2 centers) using a microspectrophotometric technique. These defects are localized in tracks surrounding the ion trajectories in which the energy is deposited by the δ rays emitted. Concerning the creation of primary defects, it has been shown that each individual track is saturated with F centers ($\simeq 4\times 10^{18}$ F centers/cm^3). From the evolution of the F center depth profiles as a function of the ion doses, using a model of saturated tracks, it has been possible to determine the radii of the tracks all along the ion trajectories. These radii, which are of the order of 7.5, 8, 14, and 32 nm at the entrance in the crystals for Ne, Ar, Kr, and Xe, respectively, increase continuously up to the values of 12, 16, 20, and 44 nm during the slowing down of the ions up to the end of the trajectories. In the wide range of energy deposition into electronic processes studied (from 0.2 to 20 MeV μm^{-1}), a continuous behavior of the primary-defect creation is observed. This seems to indicate that the same excitonic mechanism is responsible of the primary-Frenkel-pair creation in the volume of the track irradiated by the secondary electrons and other mechanisms such as Coulomb explosion or melting, which could take place in the tracks above a certain dissipated-energy threshold, must be ruled out. Finally, the specificity of damaging with ions compared with other irradiation modes (electrons or electromagnetic radiation) is mainly observed with aggregated defects. Due to the high energy density dissipated in the tracks and saturation with isolated primary defects, a great number of other primary defects are stabilized in the form of various aggregate centers in the anionic and cationic sublattices. With such a complex damage microstructure, the recombination, aggregation, and annealing mechanisms observed are nonconventional. For example, it is shown that the aggregation of F centers into F_2 centers is markedly influenced by the nature and energy of the projectile.

I. INTRODUCTION

Energetic ions penetrating matter are slowed down by momentum transfer to target atoms ("nuclear stopping"), and by excitation of the electronic system of the target ("electronic stopping"). These interaction mechanisms are rather well known at the present time, and appropriate theoretical models exist to calculate the energy depositions and ranges of ions in solids.[1,2] However, the situation is quite different for the damage resulting from the energy dissipation. In this case we have to consider the specificity of the energy deposition by ions in matter: a very high density of energy dissipated in a very short time ($\sim 10^{-14}$ sec) in a small volume surrounding the ion trajectory.

For low-energy ions ($\sim$keV/amu) when the interaction by nuclear elastic collisions dominates, this energy-localization volume is the collision-cascade volume. For higher-energy ions ($\sim$MeV/amu), the electronic stopping is preponderant, and in this case the deposited energy will be localized in a track containing the δ rays emitted from the ion trajectory that can be considered as a linear source of electrons.[3]

In most of the cases it is quite difficult to study the damage creation directly related with the energy-deposition mechanisms for various well-understandable reasons: (i) The target is generally observed at a time infinitely long compared with the time characteristic of the energy deposition. Thus depending on the nature of the target and the experimental conditions (i.e., temperature) a lot of secondary effects can take place that considerably modify the initial situation. (ii) The direct measurements that characterize the interaction volume in which the energy has been dissipated are difficult because of its microscopic size. However, in a limited number of cases a good choice of the target and the investigation technique has allowed a direct observation of the cascade volume associated with low-energy ions[4,5] or of the track in the case of high-energy heavy ions.[6]

The works presented in this paper are especially con-

 ©1990 The American Physical Society

cerned with the defect creation in the tracks surrounding the high-energy heavy ions in which a high density of energy is deposited via electronic processes. A lot of previous studies of these tracks have been carried out. However, in most of the cases the technique revealed the individual tracks after a chemical etching, which unfortunately destroys the volume containing the damage structure we want to study in connection with the energy deposition. More recently, the observation using high-resolution transmission electron microscopy of amorphized tracks in garnets bombarded with 3 GeV xenon ions,[6] illustrated the high damage level that can be expected as a result of the high energy density dissipated around the ion trajectory by electronic processes.

As for the appropriate targets that can be used for these studies, a special mention must be given to ionic crystals, and especially alkali halides. Such materials are very sensitive to electronic excitations for the creation of point defects in the anionic sublattice (color centers). This results from the rather large amount of ionic relaxation that follows any electronic change inducing a directed ionic motion of a halide ion.[7] Also, the primary defects (Frenkel pairs) as well as the aggregate–centers are well known and easily revealed using optical absorption measurements, which are very sensitive, nondestructive, and which give a quantitative evaluation of the local concentrations of defects in the tracks.[8–10] It is also interesting to remark that pure ionic crystals are not amorphized by heavy-ion bombardment. In this case the point-defect structure which subsists up to a very high level of energy deposition allows the study of some interesting effects, such as the departure of linearity in the defect production, saturation effects, and aggregation mechanisms.

Among all the alkali halides crystals we have chosen for our studies lithium fluoride (LiF), which is one of the less hygroscopic and which can be easily cleaved into thin platelets very convenient for our optical-absorption measurement technique. These crystals have been bombarded with use of the Grand Accélérateur National d'Ions Lourds (GANIL) in Caen. In order to explore a large range of electronic stopping, bombardments with Ne (40 MeV/amu), Ar (60 MeV/amu), Kr (42 MeV/amu), and Xe (27 MeV/amu) ions have been performed. Crystals bombarded with doses as low as $\sim 10^8$ ions cm^{-2} have been measured, which allows us to investigate a system with individual tracks. For crystals bombarded with higher doses up to $10^{12}-10^{13}$ ions cm^{-2}, the overlapping effects between tracks have been studied. In order to explore the defect production along the penetration depth of incident ions and compare with the electronic energy-loss depth profiles, a special microspectrophotometric technique has been developed.[10]

II. EXPERIMENTAL PROCEDURE

Thin platelets of LiF were cleaved from an ultrahigh-purity single-crystal block purchased from Quartz et Silice. The dimensions were 20 mm × 5 mm and the thickness was 0.1–0.2 mm, depending on the irradiation dose and the optical-absorption level to detect. These platelets were presented together in a metallic sample holder having the form of a small vice [Fig. 1(a)]. Using this geometry the samples were bombarded on their side as indicated in Fig. 1. The irradiations with Ne (40 MeV/amu), Ar (60 MeV/amu) Kr (42 MeV/amu), and Xe (27 MeV/amu) ions were performed at room temperature using the beam line facilities of the laboratoire CIRIL at GANIL in Caen. The current densities on the targets during the irradiations were in the range 10^8-10^9 ions cm^{-2} sec^{-1}, and the beam was scanned in order to limit the thermal effects and to obtain a homogeneously bombarded surface of 2×2 cm^2. In front of the sample the ion beam passed through a thin foil of tantalum (2.5 μm) in order to monitor the beam current and integrate the total dose using the secondary electron emission. In the case of Ne, Ar, and Kr irradiations, the tantalum foil was placed between two thin aluminum foils (12 μm) positively polarized to obtain a good secondary electron extraction. On the other hand, in the case of Xe irradiations, in order to avoid a too large degradation of the energy of incident ions, only the tantalum foil was used. This could explain some relative differences in the dose determination for Xe experiments compared with other ion experiments.

After irradiations the depth distribution profiles of point defects were measured using a microspectrophotometric technique. This technique described in more detail in a previous paper[10] consisted of scanning the whole penetration depth of the incident ions (colored zone) with the light spot of the microspectrophotometer [Fig. 1(b)]. These measurements were performed at various wavelengths corresponding to the absorption band positions of the centers responsible for the coloration, and which were the result of the energy deposition along the ion tracks by electronic interaction processes. This optical technique allows a quantitative determination of the concentration profiles of defects with a rather good spatial resolution in depth, taking into account the large penetration depths in LiF of the high-energy heavy ions used for our experiments (for Ne, $\simeq 1.4$ mm; for Ar, $\simeq 1.9$ mm; for Kr, $\simeq 0.6$ mm, and for Xe, $\simeq 0.2$ mm)

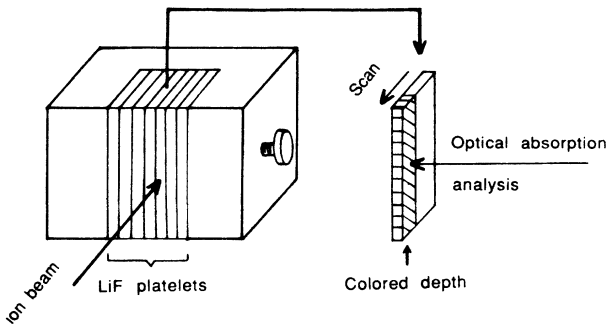

FIG. 1. Cleaved LiF platelets maintained in a small vice to perform the ion bombardments on side (a). The colored depth is subsequently analyzed in the optical-absorption microspectrophotometer to obtain the depth-distribution profiles of defects.

compared with the dimension of the light analysis spot of the microspectrophotometer (~few micrometers).

III. PRIMARY DEFECT CREATION INSIDE OF THE TRACK

As mentioned earlier, one characteristic of ionic crystals that may permit the production of directed ionic motion from a single excitation of a halide ion is the rather large amount of ionic relaxation that follows any electronic change.[7] Depending on the temperature, the primary defect in the form of a Frenkel pair resulting from this elementary electronic process can be stabilized in the lattice. At room temperature, the interstitial atoms can be stabilized in large cluster configurations when the anionic vacancies that trap electrons produce *F*-type centers. These produced *F* centers, which are very stable at room temperature, are responsible for a characteristic optical-absorption band located at 250 nm in LiF. Since the oscillator strength of the electronic transition associated with the optical absorption is known (~0.6) (Ref. 11) it is possible to calculate the *F*-center concentration from the measured surface of the absorption band, using Smakula's equation modified by Dexter.[12] In the case of LiF, the *F*-center concentrations (N_F) can be deduced from the optical-absorption measurements at room temperature using the relation

$$N_F = 9.48 \times 10^{15} \alpha_{\max} , \quad (1)$$

where $\alpha_{\max}$ is the absorption coefficient measured at the maximum of the band.

Some examples of the *F*-center concentration depth profiles measured in LiF bombarded with Ne (40 MeV/amu), Ar (60 MeV/amu), Kr (42 MeV/amu), and Xe (27 MeV/amu) ions are presented in Fig. 2. The

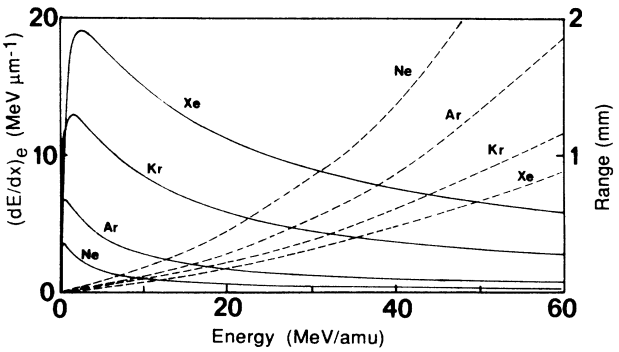

FIG. 3. Calculated electronic energy-loss profiles (solid lines) and ranges (dotted lines) of Ne, Ar, Kr, and Xe ions in LiF (Ref. 13).

shape of these profiles is comparable with the Bragg's curve, characteristic of the electronic energy losses (Fig. 3) that have been calculated using the method described by Dunlop *et al.*[13] Also the positions of the peaks at the end of the coloration profiles (1.38, 1.85, 0.60, and 0.20 mm for Ne, Ar, Kr, and Xe, respectively) are in a rather good agreement with the Bragg's peak positions in the calculated electronic energy loss profiles (1.34, 1.83, 0.63, and 0.23 mm for Ne, Ar, Kr, and Xe, respectively). However, the Bragg's peak at the end of the calculated $(dE/dx)_e$ profile is very sharp and narrow compared with the corresponding peak in the *F* center measured profile. This difference exists even after correction of the energy-loss profile, taking into account the straggling effects that somewhat widen the Bragg's peak.

The *F*-center production along the ion path in each individual track, as a function of the energy dissipated into electronic interactions, is presented in Fig. 4. The *F*-

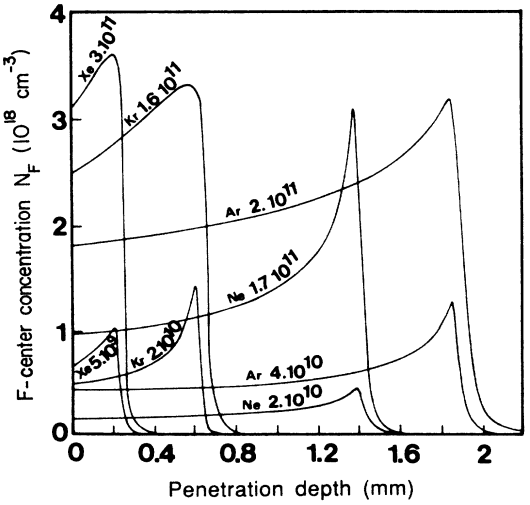

FIG. 2. Some examples of the depth-distribution profiles of *F* centers measured by optical-absorption microspectrophotometry in LiF bombarded with Ne (40 MeV/amu), Ar (60 MeV/amu), Kr (42 MeV/amu), and Xe (27 MeV/amu) ions. The fluence of ions cm^{-2} is indicated on each profile.

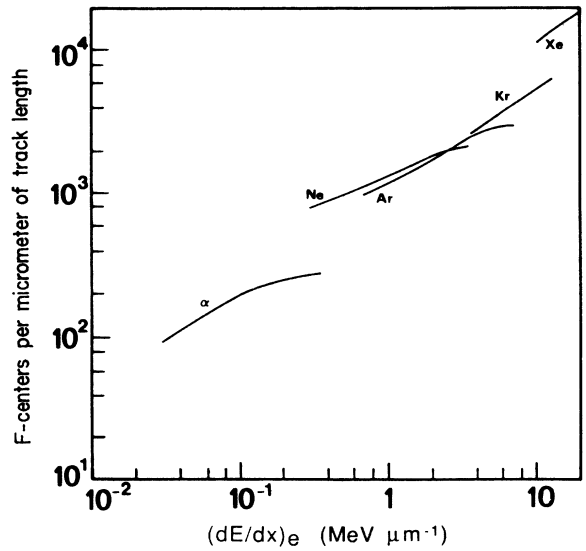

FIG. 4. *F*-center production curves along each individual track in LiF bombarded with α particles (14 MeV/amu), Ne (40 MeV/amu), Ar (60 MeV/amu), Kr (42 MeV/amu), and Xe (27 MeV/amu) ions obtained from the comparison of the measured *F*-center profiles and the calculated electronic energy-loss profiles.

center production curves presented in this figure have been obtained after a comparison of the calculated $(dE/dx)_e$ profiles and the measured F-center profiles in samples bombarded with very low ion doses ($\leq 10^{10}$ ions cm^{-2}) in order to neglect the overlapping of tracks and obtain a result characteristic of an individual track system. Also the curve obtained in a previous study of LiF bombarded with light ions such as α particles[10] is reported in Fig. 4 in order to extend the $(dE/dx)_e$ range towards low values. In the log-log scale representation used in Fig. 4, one remarks that the F-center production is linear as a function of the energy deposition along the greater part of the ion path. Only at the end of the ion trajectory, near the Bragg's peak, a departure from linearity is observed. This last effect is well marked for α, Ne, and Ar ions but becomes weak for Kr ions and is not observed for Xe ions. From the slope of the linear part of the curve for each ion one can deduce that the F-center production in each individual track is of the form

$$N_F = \left[\frac{dE}{dx}\right]_e^{0.6} . \tag{2}$$

In this relation N_F is the number of F center per unit path length and per incident ion and $(dE/dx)_e$ represents the electronic energy loss per unit path length of the ion.

Comparison of F-center concentrations at the same dE/dx values reveals some small discrepancies. The Ar curve is slightly below the Ne curve, the Kr curve is slightly above the Ar curve, and the Xe curve is more significantly shifted upwards. Two explanations can be involved: (i) a change in the F-center creation efficiency with the electronic stopping power; (ii) some differences in the ion dose measurements or in the irradiation conditions (temperature, dose rate). This last hypothesis seems more reasonable.

As for the exponent 0.6 obtained experimentally for the F-center production along the track [Eq. (2)], it includes several physical phenomena. Some are characteristic of the microscopic structure of the energy deposition inside the track and others are characteristic of the nature of the target. In a first approach, we can try to separate the different contributions by comparing the defect production with ions to those obtained with electromagnetic radiations. For example, the ^{60}Co γ rays ($\sim$1.25 MeV) interact in LiF mainly by the Compton effect. The emitted Compton electrons lose their energy in the material producing defects by the same mechanisms that the δ rays emitted in the track surrounding an energetic ion. However, in the case of γ rays, the energy is homogeneously deposited in the irradiated volume, leading to a uniform density of defects. The F-center production curve measured in LiF irradiated at room temperature with ^{60}Co γ rays is presented in Fig. 5. For an energy density (D_E) lower than about 10 megarads, the F-center production is linear in the log-log scale and we can deduce: $N_F \sim D_E^{0.8}$. Above 10 Mrads a saturation effect is observed. In fact, we have to notice that the energy density dissipated in the track surrounding a heavy ion in LiF is in all cases larger than 10 Mrads. This is supported by a previous calculation of the radial distribution of energy dissipated in the track of an α particle in LiF (Ref. 10), which shows that even for this light ion the energy density in the center of the track reaches a value of 10 Mrads or more depending on the energy of the ion. Consequently, in the case of Ne, Ar, Kr, and Xe ions, we are sure that the energy density in the greater part of the tracks is higher than 10 Mrads, which allows us to consider that each individual track is saturated with F centers. On the basis of this assumption, a model of F-center production with saturated tracks has been developed by Thevenard *et al.*[14] In this model, a saturated density of defects contained in a cylindrical volume surrounding the ion trajectory is assumed. Also when these cylinders saturated with defects overlap, the creation rate for isolated F centers is assumed to be negligible in the overlapping region. The F-center creation law obtained from this model is in the form

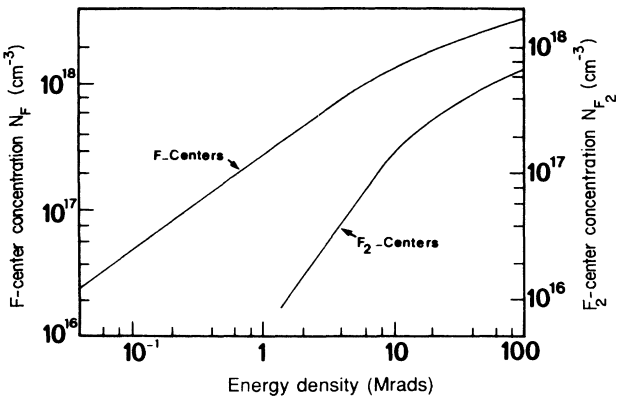

FIG. 5. F-center and F_2-center production curves in LiF irradiated at room temperature with ^{60}Co γ rays.

$$N_F = n_F[1-\exp(-\pi r^2 \Phi)] , \tag{3}$$

where N_F is the total F-center concentration obtained for an irradiation with an ion dose Φ, n_F is the saturated concentration of F centers in each individual track, and r is the radius of the track.

From the F-center depth profiles measured with Ne, Ar, Kr, and Xe ions bombarded LiF it is possible to plot the F-center concentration as a function of dose at various depths along the profiles, that is to say at various energies of the incident ions. These curves are reported in Fig. 6 for ion doses ranging from 10^9 to 10^{12} ions cm^{-2}. From the computer fitting of these curves using the relation (3), one can determine the radius r of the track saturated with F centers. These results obtained for Ne, Ar, Kr, and Xe, from the entrance face in the crystal up to the Bragg's peak near the end of the incident particle path are reported in Fig. 7. We observe that the radii of the tracks increase when the energy of the ions decreases. This is in agreement with the calculated results from the radial energy distribution due to δ-rays that propagate around the ion trajectory. In fact, the energy density in

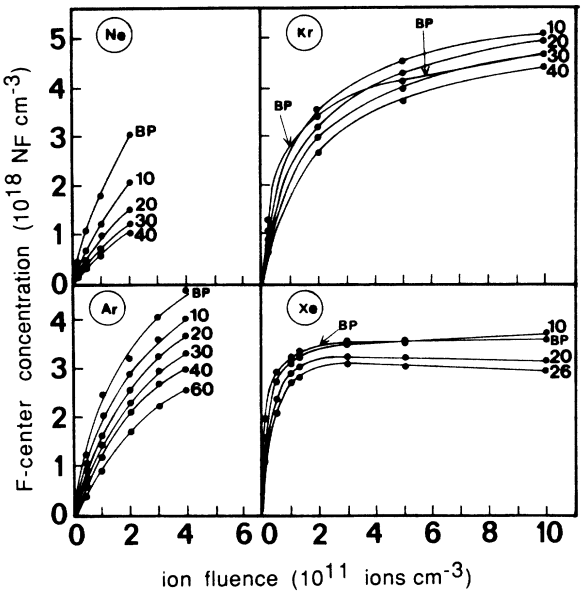

FIG. 6. F-center growth curves in LiF bombarded at room temperature with Ne, Ar, Kr, and Xe ions as a function of the ion fluence at various energies of the incident ions along the tracks. The energy is indicated on each curve in MeV/amu. BP indicates the curves obtained at the Bragg's peak.

the track due to secondary electrons increases when the energy of the particle decreases. If we assume that above a given energy deposition threshold (~ 10 Mrads in LiF) the track is saturated with defect we understand quite well the effect of increasing radius when the energy of the incident ion decreases.

Another interesting parameter deduced from the fits of the F-center growth curves in Fig. 6 is the saturation level n_F in each individual track. The value of n_F is of the order of 4×10^{18} F centers/cm^3 for all the heavy ions used in our study. It allows us to deduce the radius of the exclusion volume necessary around one F center to remain isolated, which is of the order of 4.5 nm. Taking into account the lattice parameter of LiF (a=0,4016 nm), this radius represents about ten lattice distances. It is also remarkable that the saturated concentration of F centers in the track ($n_F \simeq 4\times10^{18}$ F centers/cm^3) is comparable to the value obtained in LiF irradiated with γ rays in the saturation region (see Fig. 5: $n_F \simeq 3.3\times10^{18}$ F centers/cm^3 for an irradiation dose of 100 Mrads).

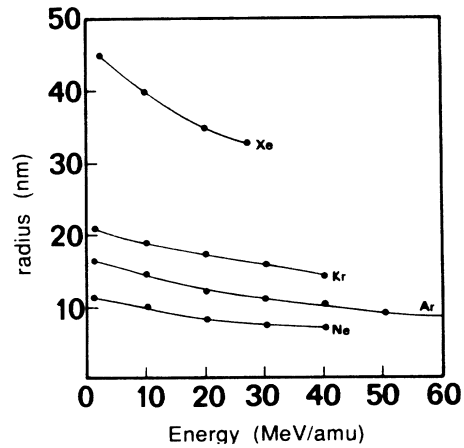

FIG. 7. Radii of the tracks in LiF as a function of the energy of the incident ions calculated from the fits of the F-center growth curves presented in Fig. 6 using the model of saturated tracks with F centers. The last point at the low-energy side of each curve corresponds to the Bragg's peak.

IV. DEFECT AGGREGATION IN THE TRACKS

The defect microstructure in the track is very complex due to the high density of energy dissipated. As mentioned before, the track is saturated with primary defects such as F centers and a great number of simple aggregated defects (F_2,F_3, . . . ,) or more complex precipitates are formed.[8,9] For this reason the study of the aggregation mechanisms in the ion tracks is quite difficult. However, the presence of some well resolved optical-absorption bands in the spectra of irradiated LiF crystals due to aggregated F center allows us to approach these effects by using the same microspectrophotometric technique to obtain the depth-distribution profiles of these centers. Such measurements have been performed for the F_2 centers that are stable at room temperature in LiF and are responsible for an absorption band located at 450 nm. Unfortunately, the oscillator strength of the F_2 centers is lower ($\simeq 0.28$) (Ref. 11) than that of F centers. For this reason the sensitivity of the optical detection of the F_2 centers is not as good as those for F centers. This effect, combined with the low production rate of F_2 centers compared to F centers, obliges us to study the F_2 center profiles at ion doses larger than those used for the F-center profile studies. For Ne, Ar, Kr, and Xe irradiated samples the lower ion doses used for the F_2-center profile studies was comprised between 1×10^{10} and 1×10^{11} ions cm^{-2}. A consequence of the use of higher ion doses for the studies of F_2-center profiles is an increase of the overlapping effect of tracks that can introduce some changes in the $F\rightarrow F_2$ formation kinetics. This effect is illustrated in Fig. 8 in which is plotted the F_2-center production measured in LiF bombarded with Ne, Ar, Kr, and Xe as a function of the electronic stopping power. We observe that the slope of the F_2-center production curve [$NF_2 \sim (dE/dx)_e^n$], along the track for each ion increases from Ne ($n \simeq 1.15$) to Xe ($n \simeq 1.50$). This evolution is different from those observed for F centers (Fig. 4) for which the exponent of the production curve along the track is constant from Ne to Xe [see Eq. (2)]. In fact, for a given ion dose, the overlapping of tracks increases from Ne to Xe due to the increase of the radius of the tracks. In the overlapping regions that are saturated with F centers, the dissipated energy can be converted only into aggregated centers. This effect can explain the increase of the F_2-center production along the track from Ne to Xe experimentally observed.

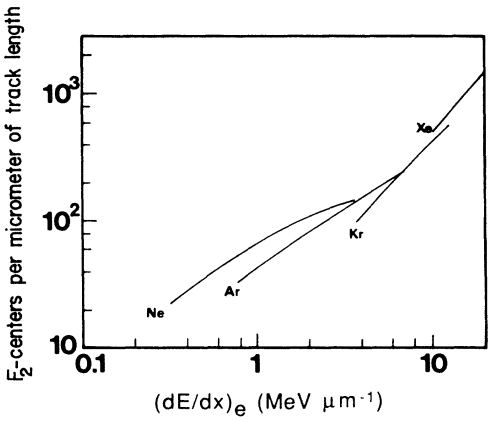

FIG. 8. F_2-center production curves along the track in LiF bombarded with Ne (40 MeV/amu), Ar (60 MeV/amu), Kr (42 MeV/amu), and Xe (27 MeV/amu) ions obtained from the comparison of the measured F_2-center profiles and the calculated electronic energy-loss profiles.

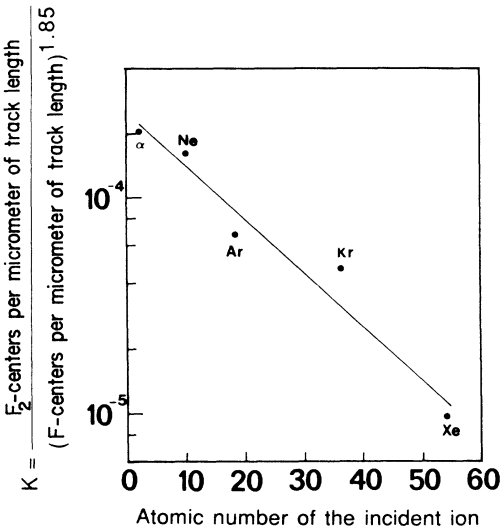

FIG. 10. Evolution of the proportionality factor K in the aggregation law for F_2 centers ($N_{F_2}=KN_F^{1.85}$) as a function of the atomic number of the incident ion.

If we assume that the separate F-center production is followed by pairing of randomly close defects to form F_2 centers we can write the relationship

$$N_{F_2}=K(N_F)^2 , \tag{4}$$

where N_F and N_{F_2} are the concentrations of F and F_2 centers, respectively, and K is a constant, the value of which is a function of the rate of energy deposition in the track since the rate controlling processes are mainly a statistical pairing of F centers and trapping of interstitials.[11] Such a relation with an exponent of 2 is obtained from the comparison of the F_2- and F-centers growth curves in the liner part before saturation (see Fig. 5) in the case of LiF irradiated with ^{60}Co γ rays. Also the relation (4) has been verified in various alkali halides irradiated with x rays or electrons and more recently Abu-Hassan *et al.*[11] have extensively discussed its validity in LiF bombarded with various energetic ions. In our experiments with high-energy heavy ions, from the comparison of the F_2- and F-center profiles we found for all the ions used that the F_2-center concentration is proportional to the F-center concentration at the power 1.8–1.9 to all along the ion tracks (Fig. 9). This experimentally found exponent is comparable to those obtained in the saturation region in crystals heavily irradiated with ^{60}Co γ rays (between 10 and 100 Mrads in Fig. 5). Thus this last result confirms the hypothesis of tracks saturated with point defects introduced previously to explain the F-center growth curves.

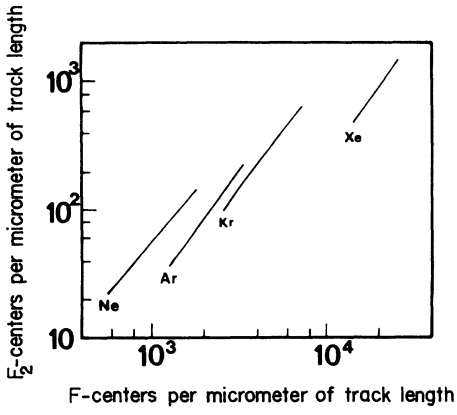

FIG. 9. Comparison of F_2- and F-center profiles measured in LiF bombarded at room temperature with Ne (40 MeV/amu), Ar (60 MeV/amu), Kr (42 MeV/amu), and Xe (27 MeV/amu) ions.

The proportionality factor K, which appears in the relation (4), depends on the nature of the incident ion, but is constant all along the track for one given ion (Fig. 9). The values of K in each individual track determined from our measurements are reported in Fig. 10 as a function of the atomic number Z of the incident ions. Also the value of K obtained in previous experiments of LiF bombarded with α particles[15] is reported in Fig. 10. Finally, in the wide range of Z investigated we found a linear decrease of K with increasing Z in a semilog plot.

V. CONCLUSION

The study of the point-defect creation at a microscopic scale directly inside of the ion track is an interesting approach in the field of radiation damage in ion bombarded materials. Such studies considerably contribute to the understanding of the specific effects of the damaging mechanisms related with the high energy deposited in the electronic system by high-energy heavy ions. From an experimental point of view, the use of ionic crystals and

especially alkali halides is very convenient, because these materials are very sensitive to electronic excitations and the resulting point-defect structures are well known. A large number of studies performed in the past on the damage creation by various energy beams: electromagnetic radiations, electrons, or ions, exist. However, in the case of ion bombarded crystals the studies generally integrated the defect created in a large number of tracks corresponding to the ion fluence and over the whole range of ions. In the present study, the use of a microspectrophotometric technique to explore the coloration in the crystal along the penetration depth of the incident ions allows a direct connection of the point-defect creation and the energy deposition in individual tracks.

The first result that emerges from the experimental study is the saturated nature of the tracks with primary defects (F centers, . . . ,). This effect, which is observed in a wide range of energy deposition into electronic excitations (from $\sim 10^{-2}$ to 20 MeV μm^{-1}) is directly connected with the localization of this energy in a small volume around the ion trajectory leading to high densities of energy depositions. One of the direct consequences of the saturated nature of the tracks is the observation of a continuous law for the F-center creation $[N_F \sim (dE/dx)_{\text{elec}}^{0.6}]$ all along the ion trajectory for light ions such as α particles as well as for heavy ions such as xenon. Finally, no sensitivity of the primary-defect creation to the electronic energy loss is observed. But a sensitivity to the volume of the track, which increases when the ions are slowed down in the target could explain our results. In fact, the local density of F centers is constant along the track because the saturation level is reached, but the absolute number of F centers increases because the damaged volume increases due to a continuous increase of the radius of the track when the ion penetrates into the target. This effect can be simply verified by comparing the ratio of the volumes of cylindrical elements of the track at the surface of the crystal and at the Bragg's peak with the ratio of the F-center concentrations at these two points deduced from the measured profiles. In the case of low dose irradiated samples, when the overlapping effect between tracks is negligible, a good agreement is observed between the two ratios previously mentioned. When the ion dose increases, the F-center profiles become more and more flat because the overlapping of tracks is larger at the Bragg's peak than at the surface of the crystal because of the difference in the radius. For high doses, the F-center profiles become completely flat, and at this stage the overlapping of tracks in the whole penetration depth of the ions leads to a homogeneous and saturated damaged volume. It is possible to estimate the density of primary defects such as F centers from the creation efficiency and saturation level measured with ionizing radiation such as γ rays. Thus no specific effect on the primary defect creation is observed inside of the track due to the very high-energy dissipated. This remark, which is verified for all the ions used, indicates that no change in the creation mechanism of primary defects takes place at a given energy threshold in the range studied (up to 30 MeV μm^{-1}). Some possible mechanisms such as Coulomb explosion in the tracks or melting due to thermal effects seem to be ruled out for the explanation of our experimental results.

If no specific effects can be found for the primary defect creation in the track, the specificity of damaging with ions appears in the aggregation mechanisms and production of complex defects. In fact the isolated F-center concentration saturates at a value around 4×10^{18} cm^{-3} but taking into account the large energy dissipated, a great number of other primary defects are created and stabilized in the form of aggregate centers. The damage microstructure in the track is very complex because of the presence of a large variety of these aggregate centers in the anionic and cationic sublattices and only a few of them are visible in the optical-absorption spectra of the irradiated crystals.[8,9] In the case of F_2-centers we observe a decrease of the proportionality factor K in the aggregation law: $N_{F_2}=KN_F^2$, from Ne to Xe. This is evidence for the presence of various other aggregate centers that are formed from the primary F centers at the expense of F_2 centers, thus increasing the complexity of the defect microstructure in the track when the dissipated energy increases. This effect is supported by some previous observations of specific aggregation mechanisms in the ion tracks. For example, in lithium fluoride bombarded with α-particles the reaction $F_2^+ + F \rightarrow F_3^+$ has been observed[9] at the difference of the normal reaction in electron of x-ray-irradiated crystals: $F_2^+ + e^- \rightarrow F_2$. Another important consequence related to the complexity and the high density of the defect microstructure in the track is the nonreversibility of certain damages when the irradiated crystals are annealed. Some large and stable clusters of alkali metal or halide atoms are present[8,15] and it is difficult to completely rebuild the lattice by annealing as it is the case in crystals not so highly damaged.

ACKNOWLEDGMENTS

We are indebted to D. Lesueur and A. Dunlap (of Laboratoire des Solides Irradiés, Ecole Polytechnique, Palaiseau) who performed the calculations of the electronic-energy-loss profiles and ranges for Ne, Ar, Kr, and Xe ions in LiF.

[1] *The Stopping and Ranges of Ions in Matter,* edited by J. F. Ziegler (Pergamon, New York, 1980).

[2] J. P. Biersack, in *Ion Beam Modification of Insulators,* edited by P. Mazzoldi and G. W. Arnold (Elsevier, Amsterdam, 1987), pp. 1–56.

[3] J. Fain, M. Monnin, and M. Montret, Radiat. Res. **57**, 379 (1974).

[4] L. M. Howe, M. H. Rainville, H. K. Haugen, and D. A.

Thompson, Nucl. Instrum. Methods **170**, 419 (1980).
[5]D. Pramanik and D. N. Seidman, Nucl. Instrum. Methods **209-210**, 453 (1983).
[6]G. Fuchs, F. Studer, E. Balanzat, D. Groult, M. Toulemonde, and J. C. Jousset, Europhys. Lett. **3**, 321 (1987).
[7]E. Sonder and W. A. Sibley, in *Point Defects in Solids,* Vol. 1 of *General and Ionic Crystals,* edited by J. H. Crawford and L. M. Slifkin (Plenum, New York, 1972), pp. 201–283.
[8]P. Thevenard, A. Perez, J. Davenas, and C. H. S. Dupuy, Phys. Status Solidi A **9**, 517 (1972).
[9]P. Thevenard, A. Perez, J. Davenas, and C. H. S. Dupuy, Phys. Status Solidi A **10**, 67 (1972).
[10]A. Perez, J. Davenas, and C. H. S. Dupuy, Nucl. Instrum. Methods **132**, 219 (1976).
[11]L. H. Abu-Hassan and P. D. Townsend, J. Phys. C **19**, 99 (1986).
[12]D. L. Dexter, Phys. Rev. **101**, 48 (1956).
[13]A. Dunlop, D. Lesieur, and J. Dural, Nucl. Instrum. Methods Phys. Res. B **42**, 182 (1989).
[14]P. Thevenard, G. Guiraud, and C. H. S. Dupuy, Radiat. Effects **32**, 83 (1977).
[15]A. Perez, Ph.D. thesis, Université Claude Bernard, Lyon, 1974.